 CMC, vol.12, no.3, pp.251-281, 2009

Three-Dimensional Solutions of Functionally Graded Piezo-Thermo-Elastic Shells and Plates Using a Modified Pagano Method

Chih-Ping Wu[1,2] **and Shao-En Huang**[2]

Abstract: A modified Pagano method is developed for the three-dimensional (3D) coupled analysis of simply-supported, doubly curved functionally graded (FG) piezo-thermo-elastic shells under thermal loads. Four different loading conditions, applied on the lateral surfaces of the shells, are considered. The material properties of FG shells are regarded as heterogeneous through the thickness coordinate, and then specified to obey an exponent-law dependent on this. The Pagano method, conventionally used for the analysis of multilayered composite elastic plates/shells, is modified to be feasible for the present analysis of FG piezo-thermo-elastic plates/shells. The modifications include that a displacement-based formulation is replaced by a mixed formulation, a set of the complex-valued solutions of the system equations is transferred to the corresponding set of real-valued solutions, a successive approximation (SA) method is adopted and introduced in the present analysis, and the propagator matrix method is developed for the heat conduction analysis and the coupled piezo-thermo-elastic analysis of the FG shells. The influence of the material-property gradient index on the field variables, induced in the FG piezo-thermo-elastic shells and plates under the thermal load, is studied.

Keywords: The Pagano method, 3D solutions, Coupled piezo-thermo-elastic effects, FG material, Heat conduction, Shells, Plates

1 Introduction

In recent decades, a class of multilayered piezoelectric structures has been developed as so-called intelligent (or smart) structures, for use in engineering applications, such as sensors for monitoring and actuators for controlling structural responses. Because this class of intelligent structures is commonly utilized in a changing thermal environment, some problems may occur due to sudden changes

[1] Corresponding author. Fax: +886-6-2370804, E-mail address: cpwu@mail.ncku.edu.tw
[2] Department of Civil Engineering, National Cheng Kung University, Tainan 70101, Taiwan, ROC

in the material properties at the interfaces between the adjacent layers, such as large thermal stresses (Crawley and Luis, 1987). Consequently, an emerging class of functionally graded (FG) piezoelectric structures has been developed in recent years. Unlike the layer-wise constant distribution of material properties through the thickness coordinate of multilayered structures, the distribution of material properties in FG structures gradually and continuously varies. However, this feature also increases the complexity and difficulty of analyzing such FG structures, especially when they operate in a changing temperature environment.

Some research into the three-dimensional (3D) analysis of multilayered piezo-thermo-elastic structures has been undertaken, building on a pioneering work (Im and Atluri, 1989) in which the effects of a piezo-actuator on a finitely deformed beam under general loads was studied. Based on a state space approach, Xu, Noor and Tang (1995) presented the 3D solutions for the static behaviors of simply-supported, multilayered plates consisting of a combination of fiber-reinforced cross-ply and piezo-thermo-elastic layers. Later, Dube, Kapuria and Dumir (1996a, b) and Zhang, Di and Zhang (2002) investigated the cylindrical bending type of deformation and stress analysis of infinitely long, simply-supported, orthotropic single-layer flat, circular cylindrical panels, and multilayered flat panels under thermo-electro-mechanical loads, respectively. Ashida and Tauchert (2001) presented a general plane-stress solution in cylindrical coordinates for a piezo-thermo-elastic plate. Literature surveys of the developments, ideas, and applications of a variety of theoretical methodologies and numerical models for the analysis of the multi-layered smart structures have been undertaken by Tauchert et al. (2000) and Tang, Noor and Xu (1996), which included most of the then-published 2D theories of piezo-thermo-elastic plates/shells.

After a close literature survey, we found that to date there are few 3D coupled thermo-electro-mechanical analyses of FG structures in comparison with those of multilayered structures. Zhong and Shang (2005) presented the exact solution of FG piezo-thermo-elastic plates, where the material properties were assumed to obey an exponent-law distribution through the thickness coordinate. Wu, Shen and Chen (2003) presented an analytical study of the piezo-thermo-elastic behavior of a FG piezoelectric cylindrical shell subject to the axisymmetric thermal or mechanical loading, where the material properties were assumed to obey a power-law dependent on the thickness coordinate. Moreover, a 3D analysis of FG magneto-electro-thermo-elastic plates using a state space approach in conjunction with the potential theory method can also be found in the literature (Chen and Lee, 2003). However, to the best knowledge of the author, the present subject, the 3D piezo-thermo-elastic analysis of simply supported, doubly curved FG shells in a changing temperature environment, can not be found in the current literature.

A review of the 3D analytical methods for multilayered and functionally graded structures made up of smart materials was undertaken by Wu, Chiu and Wang (2008), where they classified them as the Pagano (Heyliger and Brooks, 1995,1996), state space (Chen, Ding and Xu, 2001; Wu and Liu, 2007), series expansion (kapuria, Dumir and Sengupta, 1997; Kapuria, Sengupta and Dumir, 1997) and asymptotic approaches (Wu and Syu, 2006, 2007; Wu, Syu and Lo, 2007; Wu and Tsai, 2007, 2009; Tsai and Wu, 2008). Among these, the Pagano method is the most commonly applied for multilayered smart structures. However, there are some limitations when the Pagano method is applied to the analysis of FG smart plates/shells, as follows. (a) Because the material properties of FG piezoelectric plates/shells gradually vary in the thickness direction, the governing equations of FG plates/shells are a system of differential equations with variable, rather than constant, coefficients. This may mean that the Pagano method fails to directly analyze the mechanical problems of FG plates. (b) Using the Pagano method for the 3D analysis of piezoelectric plates/shells may yield a set of linearly independent solutions of system equations involving complex-valued solutions, resulting in inefficient computation for the 3D analysis. (c) A displacement-based formulation is used in the Pagano method, in which the primary displacement variables can not totally include the field variables involved in the lateral boundary conditions on the lateral surfaces and the continuity conditions at the interfaces between adjacent layers. These boundary conditions and continuity conditions can thus not be directly imposed in the solution process. (d) Using the Pagano method may turn the basic 3D equations into a system of simultaneously nonhomogeneous algebraic equations, and the computation for determining the unknowns thus becomes very time-consuming as the total number of layers constituting the plate increases.

In order to utilize the Pagano method for the analysis of FG piezoelectric plates/shells, Wu, Chen and Chiu (2009) and Wu and Lu (2009) developed a modified Pagano method for the analysis of the static and dynamic responses of simply supported, FG magneto-electro-elastic plates, respectively. The modifications to the original Pagano method are as follows. (a) A successive approximation (SA) method (Soldatos and Hadjigeorgiou, 1990) was adopted, where the FG plate is artificially divided into a certain number of individual layers with an equal and small thickness, compared with the curvature radius, for each layer. By the refinement manipulation, one may reasonably approximate the variable material coefficients of each individual layer to the constant material coefficients in an average thickness sense, so that the system of thickness-varying differential equations for each individual layer can be reduced to a system of thickness-invariant differential equations. (b) The sets of complex-valued solutions of system equations were transferred to the corresponding sets of real-valued solutions by means of Euler's formula for the purpose of

computational efficiency. (c) A mixed formulation, not the displacement-based formulation, was developed, so that both the lateral boundary conditions on the outer surfaces and the continuity conditions at the interface between adjacent layers can be directly applied. (d) A propagator matrix method was developed, so that the general solutions of system equations can be obtained layer-by-layer. These modifications made the Pagano method feasible for the 3D analysis of FG plates, and implementations showed that the computation thus became less time-consuming and independent of the total number of layers constituting the plate.

Due to the benefits of the modified Pagano method noted above, in this paper we extensively applied it to the 3D coupled analysis of simply-supported, doubly curved FG piezo-thermo-elastic shells under thermal loads. It is known that the coupling thermo-mechanical and piezoelectric effects slightly affect the distributions of thermal field variables in the spatial domain, but significantly affect the distributions of elastic and electric field variables in the spatial domain. Hence, a one-way coupled analysis of FG piezo-thermo-elastic shells is used in this work, where a heat conduction problem of FG shells under thermal loads is first analyzed, then the determined temperature distributions of the domain are used for the coupled piezo-thermo-elastic analysis of FG shells. This one-way coupled approach has been commonly used in the literature (Xu, Noor and Tang, 1995; Dube, Kapuria and Dumir, 1996a, b; Zhang, Di and Zhang, 2002; Zhong and Shang, 2005). The material properties of the shells are assumed to obey an exponent-law distribution through the thickness coordinate of the shell. Four different loading conditions on the lateral surfaces of the shell are considered. A parametric study of the influence of the material-property gradient index on the through-thickness distributions of various variables in the thermal, electric, and mechanical fields is thus undertaken.

2 Basic equations of 3D piezo-thermo-elasticity

A simply-supported, doubly curved FG piezo-thermo-elastic shell with heterogeneous material properties through the thickness coordinate is considered, as shown in Fig. 1. A set of the orthogonal curvilinear coordinates (ξ, η, ζ) is located on the middle surface of the shell. The total thickness of the shell is $2h$; a_ξ and a_η denote the curvilinear dimensions in the ξ and η directions, respectively; and R_ξ and R_η denote the curvature radii to the middle surface of the shell.

The linear constitutive equations, valid for the nature of the symmetry class of the piezo-thermo-elastic material considered, are given by

$$\sigma_i = c_{ij}\varepsilon_j - e_{ki}E_k - \alpha_i T, \tag{1}$$

$$D_l = e_{lj}\varepsilon_j + \eta_{lk}E_k + \beta_l T, \tag{2}$$

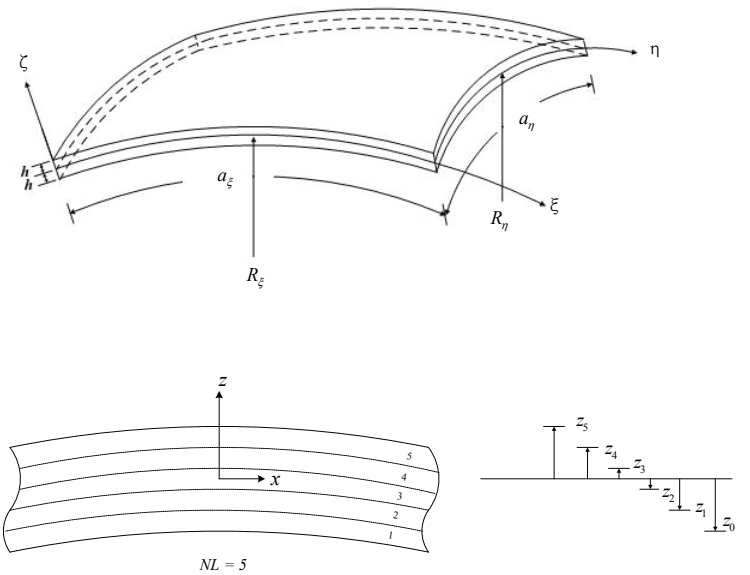

Figure 1: (a) The geometry and coordinates of a doubly curved shell; (b) The dimensionless thickness coordinates of the bottom and top surfaces of each layer constituting the FG shell

where σ_i and ε_j (i, j=1–6) are the contracted notation for the stress and strain components, respectively; D_l (l=1–3) and E_k (k=1–3) denote the electric displacement and electric field components, respectively; T denotes the temperature change; c_{ij} and η_{lk} are the elastic and dielectric permeability coefficients, respectively; and e_{ki}, α_i and β_l are the piezoelectric, stress-temperature and pyroelectric coefficients, respectively. These material properties are considered as heterogeneous through the thickness and as temperature independent (i.e., $c_{ij}(\zeta)$, $\eta_{lk}(\zeta)$, $e_{ki}(\zeta)$, $\alpha_i(\zeta)$ and $\beta_l(\zeta)$).

For an orthotropic solid, the previous material coefficients are given by

$$\mathbf{c} = \begin{bmatrix} c_{11} & c_{12} & c_{13} & 0 & 0 & 0 \\ c_{12} & c_{22} & c_{23} & 0 & 0 & 0 \\ c_{13} & c_{23} & c_{33} & 0 & 0 & 0 \\ 0 & 0 & 0 & c_{44} & 0 & 0 \\ 0 & 0 & 0 & 0 & c_{55} & 0 \\ 0 & 0 & 0 & 0 & 0 & c_{66} \end{bmatrix}, \quad \mathbf{e} = \begin{bmatrix} 0 & 0 & e_{31} \\ 0 & 0 & e_{32} \\ 0 & 0 & e_{33} \\ 0 & e_{24} & 0 \\ e_{15} & 0 & 0 \\ 0 & 0 & 0 \end{bmatrix}, \quad \boldsymbol{\alpha} = \begin{bmatrix} \alpha_1 \\ \alpha_2 \\ \alpha_3 \\ 0 \\ 0 \\ 0 \end{bmatrix}$$

$$\boldsymbol{\eta} = \begin{bmatrix} \eta_{11} & 0 & 0 \\ 0 & \eta_{22} & 0 \\ 0 & 0 & \eta_{33} \end{bmatrix}, \quad \beta = \begin{bmatrix} 0 \\ 0 \\ \beta_3 \end{bmatrix}.$$

The strain-displacement relationships are

$$\begin{Bmatrix} \varepsilon_\xi \\ \varepsilon_\eta \\ \varepsilon_\zeta \\ \gamma_{\eta\zeta} \\ \gamma_{\xi\zeta} \\ \gamma_{\xi\eta} \end{Bmatrix} = \begin{bmatrix} (1/\gamma_\xi)\,\partial_\xi & 0 & (1/\gamma_\xi R_\xi) \\ 0 & (1/\gamma_\eta)\,\partial_\eta & (1/\gamma_\eta R_\eta) \\ 0 & 0 & \partial_\zeta \\ 0 & \partial_\zeta - (1/\gamma_\eta R_\eta) & (1/\gamma_\eta)\,\partial_\eta \\ \partial_\zeta - (1/\gamma_\xi R_\xi) & 0 & (1/\gamma_\xi)\,\partial_\xi \\ (1/\gamma_\eta)\,\partial_\eta & (1/\gamma_\xi)\,\partial_\xi & 0 \end{bmatrix} \begin{Bmatrix} u_\xi \\ u_\eta \\ u_\zeta \end{Bmatrix}, \tag{3}$$

in which $\gamma_k = 1 + \zeta/R_k$ $(k = \xi, \eta)$; $\partial_i = \partial/\partial i$ $(i = \xi, \eta, \zeta)$; u_ξ, u_η and u_ζ are the displacement components.

The stress equilibrium equations without body forces are given by

$$\gamma_\eta \sigma_{xi,xi} + \gamma_\xi \tau_{\xi\eta,\eta} + \gamma_\xi \gamma_\eta \tau_{\xi\zeta,\zeta} + \left(2/R_\xi + 1/R_\eta + 3\zeta/R_\xi R_\eta\right) \tau_{\xi\zeta} = 0 \tag{4}$$

$$\gamma_\eta \tau_{\xi\eta,\xi} + \gamma_\xi \sigma_{\eta,\eta} + \gamma_\xi \gamma_\eta \tau_{\eta\zeta,\zeta} + \left(1/R_\xi + 2/R_\eta + 3\zeta/R_\xi R_\eta\right) \tau_{\eta\zeta} = 0, \tag{5}$$

$$\gamma_\eta \tau_{\xi\zeta,\xi} + \gamma_\xi \tau_{\eta\zeta,\eta} + \gamma_\xi \gamma_\eta \sigma_{\zeta,\zeta} + \left(1/R_\xi + 1/R_\eta + 2\zeta/R_\xi R_\eta\right) \sigma_\zeta - \gamma_\eta \sigma_\xi / R_\xi - \gamma_\xi \sigma_\eta / R_\eta = 0. \tag{6}$$

The equations of electrostatics for the piezo-thermo-elastic material without the electric charge density are

$$\gamma_\eta D_{\xi,\xi} + \gamma_\xi D_{\eta,\eta} + \gamma_\xi \gamma_\eta D_{\zeta,\zeta} + (\gamma_\eta/R_\xi + \gamma_\xi/R_\eta) D_\zeta = 0. \tag{7}$$

The relations between the electric field and electric potential are

$$E_k = -\Phi_{,k}/\gamma_k, \tag{8}$$

where Φ denotes the electric potential; k=ξ, η, ζ and $\gamma_\zeta = 1$.

The equations of steady state heat conduction of the piezo-thermo-elastic material without the heat generations are

$$\gamma_\eta P_{\xi,\xi} + \gamma_\xi P_{\eta,\eta} + \gamma_\xi \gamma_\eta P_{\zeta,\zeta} + (\gamma_\eta/R_\xi + \gamma_\xi/R_\eta) P_\zeta = 0. \tag{9}$$

The relations between the heat flux and temperature change are

$$P_k = -\lambda_k T_{,k}/\gamma_k, \tag{10}$$

where P_k and λ_k ($k = \xi, \eta, \zeta$) denote the heat flux and thermal conductivity, respectively.

Four different lateral surface conditions are considered, and their corresponding boundary conditions are specified, as follows:

Case 1. In the cases of closed-circuit and convection surface conditions,

$$\tau_{\xi\zeta} = \tau_{\eta\zeta} = \sigma_\zeta = \Phi = 0 \quad \text{on } \zeta = \pm h; \tag{11a}$$

and

$$-T_{,\zeta} + h_1 T = h_1 \bar{T}^- (\xi, \eta) \quad \text{on } \zeta = -h;$$

$$T_{,\zeta} + h_2 T = h_2 \bar{T}^+ (\xi, \eta) \quad \text{on } \zeta = h; \tag{11b}$$

where h_1 and h_2 denote the surface heat transfer coefficients at the bottom and top surfaces of the shell, respectively, and $\bar{T}^-$ and $\bar{T}^+$ are the applied temperature change at the bottom and top surfaces of the shell, respectively.

Case 2. In the cases of closed-circuit and prescribed temperature surface conditions,

$$\tau_{\xi\zeta} = \tau_{\eta\zeta} = \sigma_\zeta = \Phi = 0 \quad \text{on } \zeta = \pm h; \tag{12a}$$

and

$$T = \bar{T}^{\mp}(\zeta, \eta) \quad \text{on } \zeta = \mp h. \tag{12b}$$

Case 3. In the cases of open-circuit and convection surface conditions,

$$\tau_{\xi\zeta} = \tau_{\eta\zeta} = \sigma_\zeta = D_\zeta = 0 \quad \text{on } \zeta = \pm h; \tag{13a}$$

and

$$-T_{,\zeta} + h_1 T = h_1 \bar{T}^- (\xi, \eta) \quad \text{on } \zeta = -h;$$

$$T_{,\zeta} + h_2 T = h_2 \bar{T}^+ (\xi, \eta) \quad \text{on } \zeta = h. \tag{13b}$$

Case 4. In the case of open-circuit and prescribed temperature surface conditions,

$$\tau_{\xi\zeta} = \tau_{\eta\zeta} = \sigma_\zeta = D_\zeta = 0 \quad \text{on } \zeta = \pm h; \tag{14a}$$

and

$$T = \bar{T}^{\mp} (\xi, \eta) \quad \text{on } \zeta = \mp h. \tag{14b}$$

The edge boundary conditions of the shell are considered as fully simple supports, suitably grounded and isothermal, and are given as

$$\sigma_\xi = u_\eta = u_\zeta = \Phi = T = 0, \text{ at } \xi = 0 \text{ and } \xi = a_\xi; \tag{15a}$$

$$\sigma_\eta = u_\xi = u_\zeta = \Phi = T = 0, \text{ at } \eta = 0 \text{ and } \eta = a_\eta. \tag{15b}$$

There are twenty-six basic equations in the 3D piezo-thermo-elasticity, as listed in (1)–(10); and these are essentially a system of simultaneously partial differential equations with variable coefficients. In the later work of this paper, a modified Pagano method will be developed for this coupled analysis of doubly curved FG shells under thermal loads.

3 Nondimensionalization

In order to scale all the field variables within a close order of magnitude and prevent unexpected numerical instability in the computation process, we define a set of dimensionless coordinates and variables, as follows:

$$x = \frac{\xi}{\sqrt{Rh}}, \quad y = \frac{\eta}{\sqrt{Rh}}, \quad z = \frac{\zeta}{h}, \quad R_x = R_\xi/R, \quad R_y = R_\eta/R,$$

$$u = \frac{u_\xi}{\sqrt{Rh}}, \quad v = \frac{u_\eta}{\sqrt{Rh}}, \quad w = \frac{u_\zeta}{R},$$

$$\sigma_x = \frac{\sigma_\xi}{Q}, \quad \sigma_y = \frac{\sigma_\eta}{Q}, \quad \tau_{xy} = \frac{\tau_{\xi\eta}}{Q},$$

$$\tau_{xz} = \frac{\tau_{\xi\eta}}{Q\sqrt{h/R}}, \quad \tau_{yz} = \frac{\tau_{\eta\zeta}}{Q\sqrt{h/R}}, \quad \sigma_z = \frac{\sigma_\zeta R}{Qh},$$

$$D_x = D_\xi/(e\sqrt{h/R}), \quad D_y = D_\eta/(e\sqrt{h/R}), \quad D_z = D_\zeta/e,$$

$$P_x = P_\xi\sqrt{Rh}\alpha_t/(Q\lambda_t), \quad P_y = P_\eta\sqrt{Rh}\alpha_t/(Q\lambda_t), \quad P_z = P_\zeta h\alpha_t/(Q\lambda_t),$$

$$\phi = \Phi e/Qh, \quad T_t = \alpha_t T/Q, \tag{16}$$

where R, Q, e, α_t, and λ_t stand for the characteristic length, reference elastic, piezoelectric, stress-temperature, and thermal conductivity coefficients, respectively.

In the formulation, the elastic displacements (u_ξ, u_η, u_ζ), the transverse shear and normal stresses ($\tau_{\xi\zeta}$, $\tau_{\eta\zeta}$, σ_ζ), the electric flux and potential components (D_ζ, Φ) and the temperature change (T) are selected as the primary field variables. The other field variables are the secondary ones, and can be expressed in terms of the primary ones. Introducing the set of dimensionless coordinates and variables (16) and using the method of direct elimination, we obtain two sets of state space

equations, one is for the heat conduction analysis, and the other is for the coupled piezo-thermo-elastic analysis of FG shells, in terms of the primary field variables, as follows:

The set of state space equations, related to the heat conduction analysis of a FG piezo-thermo-elastic material shell, is given as

$$\frac{\partial}{\partial z}\begin{bmatrix} T_t \\ P_z \end{bmatrix} = \begin{bmatrix} 0 & l_{12} \\ l_{21} & l_{22} \end{bmatrix}\begin{bmatrix} T_t \\ P_z \end{bmatrix}, \tag{17}$$

where

$$l_{12} = -1/\lambda_z, \quad l_{21} = \left(\lambda_x h/\gamma_\xi^2 R\right)\partial_{xx} + \left(\lambda_y h/\gamma_\eta^2 R\right)\partial_{yy},$$

$$l_{22} = -\left[\left(h/R_x R\gamma_\xi\right) + \left(h/R_y R\gamma_\eta\right)\right];$$

and $\lambda_x = \lambda_\xi/\lambda_t$, $\lambda_y = \lambda_\eta/\lambda_t$, $\lambda_z = \lambda_\zeta/\lambda_t$.

The set of state space equations, related to the coupled static behavior of a FG piezo-thermo-elastic material shell, is given as

$$\frac{\partial}{\partial z}\begin{bmatrix} u \\ v \\ D_z \\ \sigma_z \\ \tau_{xz} \\ \tau_{yz} \\ \varphi \\ w \end{bmatrix} = \begin{bmatrix} k_{11} & 0 & 0 & 0 & k_{15} & 0 & k_{17} & k_{18} \\ 0 & k_{22} & 0 & 0 & 0 & k_{26} & k_{27} & k_{28} \\ 0 & 0 & k_{33} & 0 & k_{17} & k_{27} & k_{37} & 0 \\ k_{41} & k_{42} & k_{43} & k_{44} & k_{18} & k_{28} & 0 & k_{48} \\ k_{51} & k_{52} & k_{53} & k_{54} & k_{55} & 0 & 0 & k_{58} \\ k_{61} & k_{62} & k_{63} & k_{64} & 0 & k_{66} & 0 & k_{68} \\ k_{53} & k_{63} & k_{73} & k_{74} & 0 & 0 & 0 & k_{78} \\ k_{54} & k_{64} & k_{74} & k_{84} & 0 & 0 & 0 & k_{88} \end{bmatrix}\begin{bmatrix} u \\ v \\ D_z \\ \sigma_z \\ \tau_{xz} \\ \tau_{yz} \\ \varphi \\ w \end{bmatrix} - \begin{bmatrix} 0 \\ 0 \\ 0 \\ k_{49} \\ k_{59} \\ k_{69} \\ k_{79} \\ k_{89} \end{bmatrix} T_t, \tag{18}$$

where $k_{11} = h/(\gamma_\xi R R_x)$, $k_{15} = h/\tilde{c}_{55}R$, $k_{17} = -\left(\tilde{e}_{15}h/\tilde{c}_{55}\gamma_\xi R\right)\partial_x$, $k_{18} = -\left(1/\gamma_\xi\right)\partial_x$,

$$k_{22} = h/(\gamma_\eta R R_y), \quad k_{26} = h/\tilde{c}_{44}R, \quad k_{27} = -\left(\tilde{e}_{24}h/\tilde{c}_{44}\gamma_\eta R\right)\partial_y, \quad k_{28} = -\left(1/\gamma_\eta\right)\partial_y,$$

$$k_{33} = -\left[\left(h/\gamma_\xi R R_x\right) + \left(h/\gamma_\eta R R_y\right)\right],$$

$$k_{37} = \left[\left(\tilde{e}_{15}^2/\tilde{c}_{55} + \tilde{\eta}_{11}\right)h/\gamma_\xi^2 R\right]\partial_{xx} + \left[\left(\tilde{e}_{24}^2/\tilde{c}_{44} + \tilde{\eta}_{22}\right)h/\gamma_\eta^2 R\right]\partial_{yy},$$

$$k_{41} = \left[\left(\tilde{Q}_{11}/\gamma_\xi^2 R_x\right) + \left(\tilde{Q}_{21}/\gamma_\xi\gamma_\eta R_y\right)\right]\partial_x, \quad k_{42} = \left[\left(\tilde{Q}_{12}/\gamma_\xi\gamma_\eta R_x\right) + \left(\tilde{Q}_{22}/\gamma_\eta^2 R_y\right)\right]\partial_y,$$

$$k_{43} = \left(a_{21}e/Q\gamma_\xi R_x\right) + \left(a_{22}e/Q\gamma_\eta R_y\right),$$

$$k_{44} = \left(a_{11}h/\gamma_\xi R R_x\right) + \left(a_{12}h/\gamma_\eta R R_y\right) - \left(1/R_x + 1/R_y + 2hz/RR_xR_y\right)\left(h/R\gamma_\xi\gamma_\eta\right),$$

$$k_{48} = \left(\tilde{Q}_{11}/\gamma_\xi^2 R_x^2\right) + \left(\tilde{Q}_{12} + \tilde{Q}_{21}\right)/\gamma_\xi\gamma_\eta R_x R_y + \left(\tilde{Q}_{22}/\gamma_\eta^2 R_y^2\right),$$

$$k_{49} = -\left[\left(a_{31}/\gamma_\xi R_x \alpha_t\right) + \left(a_{32}/\gamma_\eta R_y \alpha_t\right)\right],$$

$$k_{51} = -\left[\left(\tilde{Q}_{11}/\gamma_\xi^2\right)\partial_{xx} + \left(\tilde{Q}_{66}/\gamma_\eta^2\right)\partial_{yy}\right], \quad k_{52} = -\left[\left(\tilde{Q}_{12} + \tilde{Q}_{66}\right)/\gamma_\xi \gamma_\eta\right]\partial_{xy},$$

$$k_{53} = -\left(a_{21} e/Q\gamma_\xi\right)\partial_x, \quad k_{54} = -\left(a_{11} h/R\gamma_\xi\right)\partial_x,$$

$$k_{55} = -\left(h/R\gamma_\xi \gamma_\eta\right)\left(2/R_x + 1/R_y + 3hz/RR_xR_y\right),$$

$$k_{58} = -\left[\left(\tilde{Q}_{11}/\gamma_\xi^2 R_x\right) + \left(\tilde{Q}_{12}/\gamma_\xi \gamma_\eta R_y\right)\right]\partial_x,$$

$$k_{59} = \left(a_{31}/\gamma_\xi \alpha_t\right)\partial_x,$$

$$k_{61} = -\left[\left(\tilde{Q}_{21} + \tilde{Q}_{66}\right)/\gamma_\xi \gamma_\eta\right]\partial_{xy}, \quad k_{62} = -\left[\left(\tilde{Q}_{66}/\gamma_\xi^2\right)\partial_{xx} + \left(\tilde{Q}_{22}/\gamma_\eta^2\right)\partial_{yy}\right],$$

$$k_{63} = -\left(a_{22} e/Q\gamma_\eta\right)\partial_y,$$

$$k_{64} = -\left(a_{12} h/R\gamma_\eta\right)\partial_y, \quad k_{66} = -\left(h/R\gamma_\xi \gamma_\eta\right)\left(1/R_x + 2/R_y + 3hz/RR_xR_y\right),$$

$$k_{68} = -\left[\left(\tilde{Q}_{21}/\gamma_\xi \gamma_\eta R_x\right) + \left(\tilde{Q}_{22}/\gamma_\eta^2 R_y\right)\right]\partial_y, \quad k_{69} = \left(a_{32}/\gamma_\eta \alpha_t\right)\partial_y,$$

$$k_{73} = e^2 b_2/Q, \quad k_{74} = ehb_1/R, \quad k_{78} = -\left[\left(a_{21} e/Q\gamma_\xi R_x\right) + \left(a_{22} e/Q\gamma_\eta R_y\right)\right],$$

$$k_{79} = -b_3 e/\alpha_t,$$

$$k_{84} = a_1 Qh^2/R^2, \quad k_{88} = -\left[\left(a_{11} h/\gamma_\xi RR_x\right) + \left(a_{12} h/\gamma_\eta RR_y\right)\right],$$

$$k_{89} = -a_3 Qh/\left(\alpha_t R\right);$$

the relevant coefficients in the previous terms of l_{ij} and k_{ij} are given in Appendix A.

The in-surface stresses, electric displacements and heat flux are dependent field variables, that can be expressed in terms of the primary variables, as follows:

$$\boldsymbol{\sigma}_1 = \mathbf{B}_1\mathbf{u} + \mathbf{B}_2 w + \mathbf{B}_3\sigma_z + \mathbf{B}_4 D_z + \mathbf{B}_5 T_t, \tag{19}$$

$$\mathbf{d} = \mathbf{B}_6\sigma_s + \mathbf{B}_7\varphi, \tag{20}$$

$$\mathbf{p} = \mathbf{B}_8 T_t, \tag{21}$$

where

$$\sigma_p = \begin{Bmatrix} \sigma_x \\ \sigma_y \\ \tau_{xy} \end{Bmatrix}, \quad \mathbf{u} = \begin{Bmatrix} u \\ v \end{Bmatrix}, \quad \sigma_s = \begin{Bmatrix} \tau_{xz} \\ \tau_{yz} \end{Bmatrix}, \quad \mathbf{d} = \begin{Bmatrix} D_x \\ D_y \end{Bmatrix}, \quad \mathbf{p} = \begin{Bmatrix} P_x \\ P_y \end{Bmatrix},$$

$$\mathbf{B}_1 = \begin{bmatrix} \left(\tilde{Q}_{11}/\gamma_\xi\right)\partial_x & \left(\tilde{Q}_{12}/\gamma_\eta\right)\partial_y \\ \left(\tilde{Q}_{21}/\gamma_\xi\right)\partial_x & \left(\tilde{Q}_{22}/\gamma_\eta\right)\partial_y \\ \left(\tilde{Q}_{66}/\gamma_\eta\right)\partial_y & \left(\tilde{Q}_{66}/\gamma_\xi\right)\partial_x \end{bmatrix}, \quad \mathbf{B}_2 = \begin{bmatrix} \left(\tilde{Q}_{11}/\gamma_\xi R_x\right) + \left(\tilde{Q}_{12}/\gamma_\eta R_y\right) \\ \left(\tilde{Q}_{21}/\gamma_\xi R_x\right) + \left(\tilde{Q}_{22}/\gamma_\eta R_y\right) \\ 0 \end{bmatrix},$$

$$\mathbf{B}_3 = \begin{bmatrix} a_{11}h/R \\ a_{12}h/R \\ 0 \end{bmatrix}, \quad \mathbf{B}_4 = \begin{bmatrix} a_{21}e/Q \\ a_{22}e/Q \\ 0 \end{bmatrix}, \quad \mathbf{B}_5 = \begin{bmatrix} a_{31}/\alpha_t \\ a_{32}/\alpha_t \\ 0 \end{bmatrix},$$

$$\mathbf{B}_6 = \begin{bmatrix} (\tilde{e}_{15}/\tilde{c}_{55}) & 0 \\ 0 & (\tilde{e}_{24}/\tilde{c}_{44}) \end{bmatrix}, \quad \mathbf{B}_7 = \begin{bmatrix} -\left(\tilde{e}_{15}^2/\tilde{c}_{55} + \tilde{\eta}_{11}\right)\partial_x/\gamma_\xi \\ -\left(\tilde{e}_{24}^2/\tilde{c}_{44} + \tilde{\eta}_{22}\right)\partial_y/\gamma_\xi \end{bmatrix},$$

$$\mathbf{B}_8 = \begin{bmatrix} -\lambda_x\partial_x/\gamma_\xi \\ -\lambda_y\partial_y/\gamma_\eta \end{bmatrix}.$$

The dimensionless form of the boundary conditions of the problem are specified as follows:

Case 1.

$$\tau_{xz} = \tau_{yz} = \sigma_z = \varphi = 0 \quad \text{on } z = \pm 1; \tag{22a}$$

and

$$-T_{t,z} + hh_1 T_t = hh_1 \bar{T}_t^-(x,y) \quad \text{on } z = -1;$$

$$T_{t,z} + hh_2 T_t = hh_2 \bar{T}_t^+(x,y) \quad \text{on } z = 1; \tag{22b}$$

where $\bar{T}_t^{\mp} = \alpha_t \bar{T}^{\mp}(\zeta,\eta)/Q$.

Case 2.

$$\tau_{xz} = \tau_{yz} = \sigma_z = \varphi = 0 \quad \text{on } z = \pm 1; \tag{23a}$$

and

$$T_t = \bar{T}_t^{\mp} \quad \text{on } z = \mp 1. \tag{23b}$$

Case 3.

$$\tau_{xz} = \tau_{yz} = \sigma_z = D_z = 0 \quad \text{on } z = \pm 1; \tag{24a}$$

and

$$-T_{t,z} + hh_1 T_t = hh_1 \bar{T}_t^-(x,y) \quad \text{on } z = -1;$$

$$T_{t,z} + hh_2 T_t = hh_2 \bar{T}_t^+(x,y) \quad \text{on } z = 1. \tag{24b}$$

Case 4.

$$\tau_{xz} = \tau_{yz} = \sigma_z = D_z = 0 \quad \text{on } z = \pm 1; \tag{25a}$$

and

$$T_t = \bar{T}_t^{\mp} \quad \text{on } z = \mp 1. \tag{25b}$$

At the edges, the following quantities are satisfied:

$$\sigma_x = v = w = \varphi = T_t = 0, \text{ at } x = 0 \text{ and } x = a_\xi/\sqrt{Rh}; \tag{26a}$$

$$\sigma_y = u = w = \varphi = T_t = 0, \text{ at } y = 0 \text{ and } y = a_\eta/\sqrt{Rh}. \tag{26b}$$

4 The modified Pagano method

4.1 The method of double Fourier series expansion

The method of double Fourier series expansion is applied to reduce the system of partial differential equations (17)–(18) to a system of ordinary differential equations. By satisfying the edge boundary conditions, we express the primary variables in the following form

$$(u, \tau_{xz}) = \sum_{\hat{m}=1}^{\infty} \sum_{\hat{n}=1}^{\infty} (u_{\hat{m}\hat{n}}(z), \quad \tau_{xz\hat{m}\hat{n}}(z)) \cos \tilde{m}x \sin \tilde{n}y, \tag{27}$$

$$(v, \tau_{yz}) = \sum_{\hat{m}=1}^{\infty} \sum_{\hat{n}=1}^{\infty} (v_{\hat{m}\hat{n}}(z), \quad \tau_{yz\hat{m}\hat{n}}(z)) \sin \tilde{m}x \cos \tilde{n}y, \tag{28}$$

$$\begin{aligned}(w, \sigma_z, \varphi, D_z, T_t, P_z) \\ = \sum_{\hat{m}=1}^{\infty} \sum_{\hat{n}=1}^{\infty} (w_{\hat{m}\hat{n}}(z), \sigma_{z\hat{m}\hat{n}}(z), \varphi_{\hat{m}\hat{n}}(z), D_{z\hat{m}\hat{n}}(z), T_{t\hat{m}\hat{n}}(z), P_{z\hat{m}\hat{n}}(z)) \sin \tilde{m}x \sin \tilde{n}y,\end{aligned} \tag{29}$$

where $\tilde{m} = \hat{m}\pi\sqrt{Rh}/a_\xi$, $\tilde{n} = \hat{n}\pi\sqrt{Rh}/a_\eta$, and $\hat{m}$ and $\hat{n}$ are the positive integers.

For brevity, the symbols of summation are omitted in the following derivation. Using the set of dimensionless coordinates and field variables (16) and substituting (27)–(29) in (17)–(18), we have the resulting equations, as follows:

$$d\mathbf{F}_t(z)/dz = \bar{\mathbf{L}}\mathbf{F}_t(z), \tag{30}$$

$$d\mathbf{F}_e(z)/dz = \bar{\mathbf{K}}\mathbf{F}_e(z) + \bar{\mathbf{G}}, \tag{31}$$

where $\mathbf{F}_t = \{T_{t\hat{m}\hat{n}}\ P_{z\hat{m}\hat{n}}\}^T$, $\mathbf{F}_e = \{u_{\hat{m}\hat{n}}\ v_{\hat{m}\hat{n}}\ D_{z\hat{m}\hat{n}}\ \sigma_{z\hat{m}\hat{n}}\ \tau_{xz\hat{m}\hat{n}}\ \tau_{yz\hat{m}\hat{n}}\ \varphi_{\hat{m}\hat{n}}\ w_{\hat{m}\hat{n}}\}^T$,
$\bar{\mathbf{G}}$ is the nonhomogeneous term calculated from the known temperature function, and is given by

$$\bar{\mathbf{G}} = (T_{t\hat{m}\hat{n}}) \begin{Bmatrix} 0 & 0 & 0 & \bar{k}_{49} & \bar{k}_{59} & \bar{k}_{69} & \bar{k}_{79} & \bar{k}_{89} \end{Bmatrix}^T,$$

$$\bar{\mathbf{L}} = \begin{bmatrix} 0 & \bar{l}_{12} \\ \bar{l}_{21} & \bar{l}_{22} \end{bmatrix},$$

$$\bar{\mathbf{K}} = \begin{bmatrix} \bar{k}_{11} & 0 & 0 & 0 & \bar{k}_{15} & 0 & \bar{k}_{17} & \bar{k}_{18} \\ 0 & \bar{k}_{22} & 0 & 0 & 0 & \bar{k}_{26} & \bar{k}_{27} & \bar{k}_{28} \\ 0 & 0 & \bar{k}_{33} & 0 & -\bar{k}_{17} & -\bar{k}_{27} & \bar{k}_{37} & 0 \\ \bar{k}_{41} & \bar{k}_{42} & \bar{k}_{43} & \bar{k}_{44} & -\bar{k}_{18} & \bar{k}_{28} & 0 & \bar{k}_{48} \\ \bar{k}_{51} & \bar{k}_{52} & \bar{k}_{53} & \bar{k}_{54} & \bar{k}_{55} & 0 & 0 & \bar{k}_{58} \\ \bar{k}_{61} & \bar{k}_{62} & \bar{k}_{63} & \bar{k}_{64} & 0 & \bar{k}_{66} & 0 & \bar{k}_{68} \\ -\bar{k}_{53} & -\bar{k}_{63} & \bar{k}_{73} & \bar{k}_{74} & 0 & 0 & 0 & \bar{k}_{78} \\ -\vec{k}_{54} & -\bar{k}_{64} & \bar{k}_{74} & \bar{k}_{84} & 0 & 0 & 0 & \bar{k}_{88} \end{bmatrix},$$

where $\bar{l}_{ij}$ and $\bar{k}_{ij}$ are given in Appendix B.

4.2 Theories of the homogeneous and nonhomogeneous linear systems

4.2.1 Theory of the homogeneous linear systems $d\mathbf{F}_t(z)/dz = \bar{\mathbf{L}}\mathbf{F}_t(z)$

Equation (30) represents the state space equations for the problem of steady state heat conduction of a simply-supported, FG shell under thermal loads, which is a system of two simultaneously homogeneous ordinary differential equations in terms of two primary variables. For a certain fixed value of thickness coordinate, the coefficients of the system equations of (30) are constants. The general solution of (30) is

$$\mathbf{F}_t = \Omega_t \mathbf{L}_t, \tag{32}$$

where $\mathbf{L}_t$ is a 2x1 matrix of arbitrary constants; Ω_t is a fundamental matrix of (30) and is formed by two linearly independent solutions in the form of $\Omega_t = [\Omega_{1t}, \quad \Omega_{2t}]$, $\Omega_{it} = \Lambda_i e^{\lambda_i z}$ (i=1, 2); and λ_i and Λ_i are the eigenvalues and their corresponding eigenvectors of the coefficient matrix $\bar{\mathbf{L}}$ in (30).

If the coefficient matrix $\bar{\mathbf{L}}$ has a complex eigenvalue λ_1 (i.e., $\lambda_1 = Re(\lambda_1) + iIm(\lambda_1)$), then its complex conjugate λ_2 (i.e., $\lambda_2 = Re(\lambda_1) - iIm(\lambda_1)$) is also an eigenvalue of $\bar{\mathbf{L}}$ due to the fact that all of the coefficients of $\bar{\mathbf{L}}$ are real. In addition, $\Lambda_{1,2} = Re(\Lambda_1) \pm iIm(\Lambda_1)$ are the corresponding eigenvectors of the complex conjugate pair $\lambda_{1,2}$. Although there is nothing wrong with these two complex-valued solutions in (30), we replace them with two linearly independent solutions involving only real-valued quantities in order to achieve more efficient computational performance. Using Euler's formula these complex-valued solutions are replaced with the real-valued solutions, and are given by

$$\Omega_1 = e^{Re(\lambda_1)z}\left[Re\left(\Lambda_1\right)\cos\left(Im\left(\lambda_1\right)z\right) - Im\left(\Lambda_1\right)\sin\left(Im\left(\lambda_1\right)z\right)\right], \tag{33}$$

$$\Omega_2 = e^{Re(\lambda_1)z}\left[Re\left(\Lambda_1\right)\sin\left(Im\left(\lambda_1\right)z\right) + Im\left(\Lambda_1\right)\cos\left(Im\left(\lambda_1\right)z\right)\right]. \tag{34}$$

On the basis of the previous set of linearly independent real-valued solutions, a propagator matrix method can be developed for the present analysis of multilayered shells, and it can be extended to the analysis of FG shells using a successive approximation method (Soldatos and Hadjigeorgiou, 1990), where the shell is artificially divided into a finite number (*NL*) of individual layers with an equal and small thickness for each layer, compared with the curvature radius, as well as with constant material properties, determined in an average thickness sense. The exact 3D solutions of the temperature change in the FG shell can thus be gradually approached by increasing the number of individual layers. It is noted that the present solution process can be performed layer-by-layer, and the computational performance is independent of the total number of individual layers. Consequently, the implementation of the present approach is much less time-consuming than usual.

4.2.2 Theory of the nonhomogeneous linear system $d\mathbf{F}_e(z)/dz = \bar{\mathbf{K}}\mathbf{F}_e(z) + \bar{\mathbf{G}}$

Equation (31) represents the state space equations for the static behaviors of a simply-supported, FG piezo-thermo-elastic shell under thermal loads, applied on the lateral surfaces. That is a system of eight simultaneously nonhomogeneous ordinary differential equations in terms of eight primary variables. The general solution of (31) is

$$\mathbf{F}_e = \Omega_e \mathbf{L}_e + \bar{\mathbf{F}}_e, \tag{35}$$

where $\mathbf{L}_e$ is a 8x1 matrix of arbitrary constants; Ω_e is a fundamental matrix of (31), and is formed by eight linearly independent solutions in the form of $\Omega_e = [\Omega_{1e}, \quad \Omega_{2e}, \cdots, \quad \Omega_{8e}]$, $\Omega_{ie} = \Lambda_i e^{\lambda_i z}$ (i=1, 2, …, 8); λ_i and Λ_i are the eigenvalues and their corresponding eigenvectors of the coefficient matrix $\bar{\mathbf{K}}$ in (31), respectively; and $\bar{\mathbf{F}}_e$ is the particular solution of (31) and $\bar{\mathbf{F}}_e = -\bar{\mathbf{K}}^{-1}\bar{\mathbf{G}}$. Again, if the coefficient matrix $\bar{\mathbf{K}}$ has a certain pair of complex conjugate eigenvalues, their corresponding complex-valued eigenvectors will be transferred to a pair of real-valued eigenvectors using (33)–(34). Subsequently, an SA method in conjunction with the propagator matrix method will be developed in the following sections, and applied to the coupled piezo-thermo-elastic analysis of FG shells.

4.3 The successive approximation method

In this paper, the material properties of FG piezo-electro-elastic shells are assumed to obey an exponent-law distribution through the thickness coordinate, and are given by

$$g_{ij}(z) = g_{ij}^{(b)} e^{\kappa_p[(z+1)/2]}, \tag{36}$$

where the superscript b in the parentheses denotes the bottom surface of the shell; and κ_p denotes the material-property gradient index, which represents the degree of the material gradient along the thickness coordinate. It is noted that $\kappa_p = 0$ corresponds to the homogeneous material, $\kappa_p < 0$ to the graded soft material, and $\kappa_p > 0$ to the graded stiff material. Because the material properties of FG plates vary along the thickness coordinate, resulting in a variant coefficient matrix in the system equations (30)–(31), the conventional Pagano method can not be directly applied to this coupled analysis of FG shells. A successive approximation method is thus adopted to make the present approach feasible. In the SA method, the FG shell was artificially divided into an *NL*-layered shell with a small thickness and homogeneous material properties for each layer. For a typical m^{th}-layer, the material properties $g_{ij}^{(m)}$ are regarded as constants, and determined in an average thickness sense, as follows:

$$\begin{aligned} g_{ij}^{(m)} &= \frac{1}{\Delta z_m}\int_{z_{m-1}}^{z_m} g_{ij}(z)\,dz \\ &= \frac{2g_{ij}^{(b)}e^{0.5\kappa_p}}{\Delta z_m \kappa_p}\left[e^{(0.5\kappa_p z_m)} - e^{(0.5\kappa_p z_{m-1})}\right], \end{aligned} \tag{37}$$

where $\Delta z_m = z_m - z_{m-1}$.

By means of (37), the present modified Pagano method can be extensively applied to the coupled analysis of FG shells. Increasing the number of artificial layers (*NL*), we can approximate the exact solutions of the present coupled analysis of FG piezo-thermo-electric shells to any desired accuracy.

4.4 The propagator matrix method

As we noted above, the modified Pagano method can be applied to the heat conduction and the coupled piezo-thermo-elastic analysis of FG shells under thermal loads using (37). The through-thickness distribution of material properties of the FG shell are modified as the layerwise Heaviside functions, and these are given by

$$g_{ij}(z) = \sum_{m=1}^{NL} g_{ij}^{(m)}\left[H(z - z_{m-1}) - H(z - z_m)\right], \tag{38}$$

where *NL* denotes the total number of the artificial layers constituting the shell; $g_{ij}^{(m)}$ refers to the coefficients of c_{ij}, e_{ij}, q_{ij}, η_{ij}, d_{ij} and μ_{ij} of the m^{th}-layer in general; $H(z)$ is the Heaviside function; and z_{m-1} and z_m are the dimensionless distances, measured from the middle surface of the shell to the bottom and top surfaces of the m^{th}-layer, respectively.

A propagator matrix method for the heat conduction and coupled piezo-thermo-elastic analyses of the *NL*-layered shells is then developed, as follows.

4.4.1 Heat conduction analysis

According to (32), we can write the general solution for the heat conduction equations of the m^{th}-layer in the form of

$$\mathbf{F}_t^{(m)}(z) = \Omega_t^{(m)}(z)\mathbf{L}_t^{(m)}. \tag{39}$$

As $z = z_{m-1}$, according to (39) we obtain

$$\mathbf{L}_t^{(m)} = \left[\Omega_t^{(m)}(z_{m-1})\right]^{-1}\mathbf{F}_{t(m-1)}, \tag{40}$$

where $\mathbf{F}_{t(m-1)}$ denotes the vector of primary variables in the thermal field at the interface between the $(m\text{-}1)^{th}$ and m^{th}-layers, and $\mathbf{F}_{t(m-1)} = \mathbf{F}_t^{(m)}(z = z_{m-1})$.
As $z = z_m$, using (39) and (40), we obtain

$$\mathbf{F}_{t(m)} = \mathbf{R}_{t(m)}\mathbf{F}_{t(m-1)}, \tag{41}$$

where $\mathbf{R}_{t(m)} = \Omega_t^{(m)}(z_m)\left[\Omega_t^{(m)}(z_{m-1})\right]^{-1}$.
By analogy, the vectors of primary variables in the thermal field between the top and bottom surfaces of the shell (i.e., $\mathbf{F}_{t(NL)}$ and $\mathbf{F}_{t(0)}$) are linked by

$$\begin{aligned}\mathbf{F}_{t(NL)} &= \mathbf{R}_{t(NL)}\mathbf{F}_{t(NL-1)} \\ &= \left(\prod_{m=1}^{NL}\mathbf{R}_{t(m)}\right)\mathbf{F}_{t(0)}\end{aligned}, \tag{42}$$

where $\prod_{m=1}^{NL}\mathbf{R}_{t(m)} = \mathbf{R}_{t(NL)}\mathbf{R}_{t(NL-1)}\cdots\mathbf{R}_{t(2)}\mathbf{R}_{t(1)}$.
Equation (42) represents a set of two simultaneous algebraic equations. Imposing the thermal boundary conditions on the lateral surfaces, we may determine the other unknown primary variables on the lateral surfaces. Afterwards, the primary variables through the thickness coordinate of the shell can be obtained by

$$\begin{aligned}\mathbf{F}_t^{(m)}(z) &= \Omega_t^{(m)}(z)\left[\Omega_t^{(m)}(z_{m-1})\right]^{-1}\mathbf{F}_{t(m-1)} \\ &= \Omega_t^{(m)}(z)\left[\Omega_t^{(m)}(z_{m-1})\right]^{-1}\left(\prod_{i=1}^{m-1}\mathbf{R}_{t(i)}\right)\mathbf{F}_{t(0)}\end{aligned}. \tag{43}$$

Once the primary variables in the thermal field, which vary through the thickness of the plate, are determined, the corresponding set of dependent variables in the thermal field can then be obtained using (21).

4.4.2 Coupled piezo-thermo-elastic analysis

According to (35), we obtain the general solution for the coupled piezo-thermo-elastic equations of the m^{th}-layer in the form of

$$\mathbf{F}_e^{(m)}(z) = \Omega_e^{(m)}(z)\,\mathbf{L}_e^{(m)} + \bar{\mathbf{F}}_e^{(m)}, \tag{44}$$

where $\bar{\mathbf{F}}_e^{(m)} = -\left(\mathbf{K}^{(m)}\right)^{-1}\bar{\mathbf{G}}^{(m)}$.
As $z = z_{m-1}$, according to (44) we obtain

$$\mathbf{L}_e^{(m)} = \left[\Omega_e^{(m)}(z_{m-1})\right]^{-1}\left(\mathbf{F}_{e(m-1)} - \bar{\mathbf{F}}_e^{(m)}\right), \tag{45}$$

where $\mathbf{F}_{e(m-1)}$ denotes the vector of primary field variables at the interface between the (m-1)th and m^{th}-layers; $\mathbf{F}_{e(m-1)} = \mathbf{F}_e^{(m)}(z = z_{m-1})$.
As $z = z_m$, using (44) and (45), we obtain

$$\mathbf{F}_{e(m)} = \mathbf{R}_{e(m)}\mathbf{F}_{e(m-1)} + \bar{\mathbf{F}}_p^{(m)}, \tag{46}$$

where $\mathbf{R}_{e(m)} = \Omega_e^{(m)}(z_m)\left[\Omega_e^{(m)}(z_{m-1})\right]^{-1}$ and $\bar{\mathbf{F}}_p^{(m)} = \left(1 - \mathbf{R}_{e(m)}\right)\bar{\mathbf{F}}_e^{(m)}$.
By analogy, the vectors of primary variables in the elastic and electric fields between the top and bottom surfaces of the plate (i.e., $\mathbf{F}_{e(NL)}$ and $\mathbf{F}_{e(0)}$) are linked by

$$\begin{aligned}\mathbf{F}_{e(NL)} &= \mathbf{R}_{e(NL)}\mathbf{F}_{e(NL-1)} + \bar{\mathbf{F}}_p^{(NL)} \\ &= \left(\prod_{m=1}^{NL}\mathbf{R}_{e(m)}\right)\mathbf{F}_{e(0)} + \bar{\mathbf{P}}.\end{aligned} \tag{47}$$

where

$$\bar{\mathbf{P}} = \bar{\mathbf{F}}_p^{(NL)} + \mathbf{R}_{e(NL)}\bar{\mathbf{F}}_p^{(NL-1)} + \mathbf{R}_{e(NL)}\mathbf{R}_{e(NL-1)}\bar{\mathbf{F}}_p^{(NL-2)} + \cdots + \left(\prod_{m=2}^{NL}\mathbf{R}_{e(m)}\right)\bar{\mathbf{F}}_p^{(1)},$$

$$\prod_{m=1}^{NL}\mathbf{R}_{e(m)} = \mathbf{R}_{e(NL)}\mathbf{R}_{e(NL-1)}\cdots\mathbf{R}_{e(2)}\mathbf{R}_{e(1)}.$$

Equation (47) represents a set of eight simultaneous algebraic equations. Imposing the prescribed conditions on the lateral surfaces, we may determine the other unknown primary variables in the elastic and electric fields on the lateral surfaces.

Afterwards, these primary variables through the thickness coordinate of the shell can be obtained by

$$\mathbf{F}_e^{(m)}(z) = \Omega_e^{(m)}(z)\left[\Omega_e^{(m)}(z_{m-1})\right]^{-1}\left(\mathbf{F}_{e(m-1)} - \bar{\mathbf{F}}_e^{(m)}\right) + \bar{\mathbf{F}}_e^{(m)}. \tag{48}$$

Once the primary variables, varied through the thickness of the plate, are determined, the corresponding set of dependent variables in the elastic and electric fields can then be obtained using (19)–(20).

5 Illustrative examples

5.1 Single-layer homogeneous piezo-thermo-elastic shells

The present formulation for the coupled piezo-thermo-elastic analysis of FG shells can be reduced to that of FG plates by letting $1/R_\xi = 1/R_\eta = 0$. For comparison purposes, the exact 3D solutions, obtained by Dube et al. (1996a) for the coupled piezo-thermo-elastic analysis of simply-supported, single-layer homogeneous plates with closed-circuit surface conditions and under a cylindrical bending type of thermal load, are used to validate the accuracy of the present modified Pagano method, where $\kappa_p = 0$. The plate is considered to be composed of cadmium selenide polarized perpendicular to its mid-plane. The material properties of this crystal are given in Table 1. The lateral surface conditions of the plates are considered as Cases 1 and 3 (i.e., (11) and (13)) in Tables 2 and 3, respectively. The thermal load applied on the lateral surfaces are given as $\bar{T}^- = 0$ and $\bar{T}^+ = T_0 \sin\left(\pi\xi/a_\xi\right)$. The dimensionless variables are denoted as the same forms used in Dube et al. (1996a), and given as follows:

$$(\bar{u}, \bar{w}) = \frac{100}{2hS^2\alpha_\xi T_0}\left(Su_\xi, u_\zeta\right),$$

$$(\bar{\sigma}_x, \bar{\sigma}_y, \bar{\sigma}_z, \bar{\tau}_{xz}) = \left(S^2\sigma_\xi, \sigma_\eta, S^4\sigma_\zeta, S^3\tau_{\xi\zeta}\right)/Y_\xi\alpha_\xi T_0,$$

$$\bar{D}_z = D_\zeta/|d_1|Y_\xi\alpha_\xi T_0, \quad \bar{\varphi} = |d_1|\varphi/2h\alpha_\xi T_0, \quad \bar{T} = T/T_0, \tag{49}$$

where $S = a_\xi/2h$; and Y_ξ α_ξ and d_1 are the Young's modulus, thermal expansion coefficient and piezoelectric coefficient in direction ξ, respectively.

Tables 2 and 3 show that the present solutions of elastic, electric and thermal field variables, induced in the single-layer homogeneous piezo-thermo-elastic plates with the surface conditions of Cases 1 and 3, respectively. The accuracy of the present modified Pagano method is validated by comparing the present solutions with the available 3D solutions (Dube et al., 1996a). It is seen in Tables 2 and 3 that the present solutions are in excellent agreement with these earlier 3D solutions through a wide range, from S=2 (thick plates) to S=20 (thin plates).

Table 1: Material properties of the cadmium selenide material

c_{11} (Gpa)	74.1	η_{11} (C^2/Nm^2)	82.5e-12
c_{22}	74.1	η_{22}	82.5e-12
c_{33}	83.6	η_{33}	90.2e-12
c_{12}	45.2	α_1 (N/Km^2)	0.621e+06
c_{13}	39.3	α_2	0.621e+06
c_{23}	39.3	α_3	0.551e+06
c_{44}	13.17	β_3 (C/Km^2)	-2.94e-06
c_{55}	13.17	α_ξ	4.396e-06
c_{66}	14.45	d_1 (C/N)	-3.9238e-12
e_{31} (C/m^2)	-0.160	$2hh_1$ (1/m)	0.2
e_{32}	-0.160	$2hh_2$ (1/m)	2.0
e_{33}	0.347	Y_ξ (Gpa)	42.785
e_{24}	0.0	$\lambda_\zeta/\lambda_\xi$	1.5
e_{15}	-0.138		

5.2 Functionally graded piezo-thermo-elastic plates

A coupled analysis of FG piezo-thermo-elastic plates with closed- and open-circuit surface conditions subjected to a sinusoidally distributed temperature change on the top surface of the plate is considered in Table 4. The exact 3D solutions of this problem, obtained by Zhong and Shang (2005) using the state space method, were used to validate the accuracy and convergence rate of this method. The geometric parameters are taken as $a_\xi = a_\eta = 1m$ and $2h = 0.1m$. The material properties of the plates are assumed to obey an exponent-law dependent on the thickness coordinate, and are given as (36) with $\kappa_p = 1$, where the reference material properties on the bottom surface are identical to those used in Example 5.1, and given in Table 1. The applied sinusoidally distributed temperature change in Table 4 is given as

$$\bar{T}^+ = T_0 \sin\frac{\hat{m}\pi\xi}{a_\xi} \sin\frac{\hat{n}\pi\eta}{a_\eta}, \tag{50}$$

where $\hat{m} = \hat{n}$=1, T_0=1°K.

Table 4 shows the present results of a variety of variables in the mechanical, electric and thermal fields induced at a particular point ($\xi = a_\xi/4, \eta = a_\eta/4, \zeta = -h/2$) in the FG plates with closed-circuit (Case 2) and open-circuit (Case 4) surface conditions, respectively. It is shown that the present solutions converge rapidly, and these are in excellent agreement with the 3D solutions available in the literature (Zhong and Shang, 2005). The relative errors of the present 32-layered solutions

Table 2: The elastic, electric and thermal field variables in a single-layer piezoelectric plate under the thermal load of Case 1

S	Theories	$\bar{u}(0,-h)$	$\bar{w}(a\xi/2,0)$	$10^2\bar{\sigma}_x(a\xi/2,h)$	$\bar{\sigma}_x(a\xi/2,h)$	$10^2\bar{\sigma}_z(a\xi/2,0)$	$10^2\bar{\tau}_{xz}(0,-h/2)$	$10^4\bar{\varphi}(a\xi/2,h)$	$\bar{D}_z(a\xi/2,h)$	$\bar{T}(a\xi/2,h)$
2	Present	-13.368	4.8325	-6.2361	-0.6380	1.7586	1.6597	8.9457	-1.6220	0.6356
	Exact solution	-13.37	4.832	-6.236	-0.6380	1.759	1.660	8.946	-1.622	0.6357
4	Present	-26.603	3.4845	-11.045	-0.8067	3.3347	3.1757	7.4383	-2.4982	0.8069
	Exact solution	-26.60	3.485	-11.05	-0.8067	3.335	3.176	7.438	-2.498	0.8070
6	Present	-31.387	2.8910	-12.769	-0.8634	3.9003	3.7199	6.3537	-2.8216	0.8645
	Exact solution	-31.38	2.891	-12.77	-0.8634	3.900	3.720	6.354	-2.822	0.8646
10	Present	-34.416	2.5001	-13.859	-0.8987	4.2579	4.0639	5.5794	-3.0278	0.9004
	Exact solution	-34.41	2.500	-13.86	-0.8987	4.258	4.064	5.579	-3.028	0.9004
20	Present	-35.845	2.3126	-14.374	-0.9152	4.4265	4.2258	5.1949	-3.1254	0.9172
	Exact solution	-35.84	2.313	-14.37	-0.9152	4.426	4.226	5.195	-3.125	0.9172

Table 3: The elastic, electric and thermal field variables in a single-layer piezoelectric plate under the thermal load of Case 3

S	Theories	$\bar{u}\left(0,-h\right)$	$\bar{w}\left(a_{\xi}/2,0\right)$	$10^{3}\bar{\sigma}_{x}\left(a_{\xi}/2,h\right)$	$\bar{\sigma}_{y}\left(a_{\xi}/2,h\right)$	$10^{4}\bar{\sigma}_{z}\left(a_{\xi}/2,0\right)$	$10^{3}\bar{\tau}_{xz}\left(0,-h/2\right)$	$10^{3}\bar{\varphi}\left(a_{\xi}/2,h\right)$	$10^{4}\bar{D}_{z}\left(a_{\xi}/2,h\right)$	$\bar{T}\left(a_{\xi}/2,h\right)$
2	Present	-13.178	4.7723	-13.089	-0.62052	38.897	3.6936	-5.2859	-3313.89	0.63556
	Exact solution	-13.18	4.772	-13.09	-0.6205	NA	NA	-5.286	NA	0.6357
4	Present	-25.937	3.4721	-9.9985	-0.78597	31.03	2.9645	-8.8696	-1608.22	0.8069
	Exact solution	-25.94	3.472	-9.998	-0.786	NA	NA	-8.87	NA	0.807
6	Present	-30.534	2.8862	-8.0718	-0.84185	24.961	2.3837	-10.146	-840.87	0.86452
	Exact solution	-30.53	2.886	-8.071	-0.8419	NA	NA	-10.15	NA	0.8646
10	Present	-33.444	2.4986	-6.7202	-0.8767	20.578	1.9622	-10.952	-331.53	0.9004
	Exact solution	-33.44	2.499	-6.718	-0.8767	NA	NA	-10.95	NA	0.9004
20	Present	-34.816	2.3123	-6.0578	-0.89303	18.391	1.7489	-11.332	-86.28	0.9172
	Exact solution	-34.81	2.312	-6.051	-0.893	NA	NA	-11.33	NA	0.9172

Table 4: The elastic, electric and thermal field variables at a point ($\xi = a_\xi/4$, $\eta = a_\eta/4$, $\zeta = -h/2$) in an FG piezo-thermo-elastic plate under a sinusoidally distributed temperature change (S=10 and $\kappa_p = 1$)

Surface conditions	Theories	u_ξ	u_ζ	Φ	$\tau_{\xi\zeta}$	σ_ζ	D_ζ	σ_ξ	$\tau_{\zeta\eta}$	D_ξ
Case2	Present $NL = 4$	-3.03E-07	2.26E-06	3.42E+02	-1.77E+03	-6.46E+01	-2.02E-06	-3.23E+04	-3.53E+04	-9.71E-08
	12	-2.94E-07	2.38E-06	3.49E+02	-1.12E+03	-1.09E+02	-2.02E-06	-3.53E+04	-3.42E+04	-1.06E-07
	20	-2.93E-07	2.39E-06	3.50E+02	-1.07E+03	-1.12E+02	-2.02E-06	-3.55E+04	-3.42E+04	-1.07E-07
	32	-2.93E-07	2.39E-06	3.50E+02	-1.05E+03	-1.14E+02	-2.02E-06	-3.56E+04	-3.41E+04	-1.07E-07
	100	-2.93E-07	2.39E-06	3.50E+02	-1.04E+03	-1.14E+02	-2.02E-06	-3.56E+04	-3.41E+04	-1.08E-07
	Exact solution	NA	NA	NA	NA	NA	NA	NA	NA	NA
Case 4	Present $NL = 4$	-2.87E-07	2.29E-06	4.72E+02	-1.80E+03	-6.67E+01	-2.51E-08	-3.04E+04	-3.35E+04	-1.41E-07
	12	-2.78E-07	2.41E-06	4.79E+02	-1.15E+03	-1.11E+02	-2.51E-08	-3.35E+04	-3.24E+04	-1.50E-07
	20	-2.78E-07	2.42E-06	4.79E+02	-1.10E+03	-1.15E+02	-2.51E-08	-3.38E+04	-3.24E+04	-1.51E-07
	32	-2.77E-07	2.43E-06	4.79E+02	-1.08E+03	-1.16E+02	-2.51E-08	-3.39E+04	-3.23E+04	-1.51E-07
	100	-2.77E-07	2.43E-06	4.79E+02	-1.07E+03	-1.17E+02	-2.51E-08	-3.39E+04	-3.23E+04	-1.51E-07
	Exact solution	-2.77E-07	2.43E-06	4.79E+02	-1.07E+03	-1.17E+02	-2.51E-08	-3.39E+04	-3.23E+04	-1.51E-07

are less than 1% in comparison with the 3D available solutions.

5.3 Functionally graded piezo-thermo-elastic shells

A coupled analysis of FG piezo-thermo-elastic shells with surface conditions of Cases 1–3 is considered in Figs. 2–4, respectively, where the applied temperature change on the top surface of the shell is taken as $\bar{T}^{+} = T_0 \sin\left(\pi\xi/a_\xi\right)\sin\left(\pi\eta/a_\eta\right)$. The geometric parameters of the plates are $a_\xi/2h = a_\eta/2h = 10$ and $R_\xi/a_\xi = R_\eta/a_\eta = 5$. The dimensionless variables are identical to those used in Example 5.1, and the material-property gradient index κ_p is taken as κ_p=-3.0, -1.5, 0.0, 1.5, 3.0. The present 32-layered solutions for the through-thickness distributions of various variables in the electric, elastic and thermal fields, induced in the shells with three different surface conditions (i.e., Cases 1–3), are presented in Figs. 2–4, respectively. Figs. 2(a)–4(a) show that the through-thickness distributions of the temperature change appear to be linear in the cases of homogeneous shells (i.e., κ_p=0). However, the distributions become higher-degree polynomials when the homogeneous shells become graded stiff shells (κ_p>0) or graded soft shells (κ_p<0). It is observed from Figs. 2 and 4 that the through-thickness distributions of temperature change and mechanical variables for the shells with closed-circuit and convection surface conditions (Case 1) are very similar to those of the shells with open-circuit and convection surface conditions (Case 3); whereas the distributions of electric potential and normal electric displacement are quite different for the shells with surface conditions of Cases 1 and 3. Figs. 2–4 show that the influence of the material-property gradient index κ_p on the field variables is significant. It is also seen from Figs. 2(d, e, f)–5(d, e, f) that the prescribed boundary conditions on the lateral surfaces of the shell are exactly satisfied.

Fig. 5 shows the variations of the through-thickness distributions of various field variables, induced in the shells with the span-thickness ratio (S). The shells with the surface conditions of Case 4 and under a sinusoidally distributed temperature change are considered, where the values of various parameters are taken as $S = a_\xi/2h = a_\eta/2h$=5, 10, 20; $R_\xi/a_\xi = R_\eta/a_\eta = 5$; and $\kappa_p = 1$. It is shown that the variations of the through-thickness distributions of the temperature change with the span-thickness ratio, unlike those of other variables in the elastic and electric fields, are insignificant. The magnitudes of the temperature change and the in-surface elastic displacement induced in the shells get larger as the shells become thinner; whereas those of transverse stress, electric potential and electric normal displacement get larger as the shells become thicker.

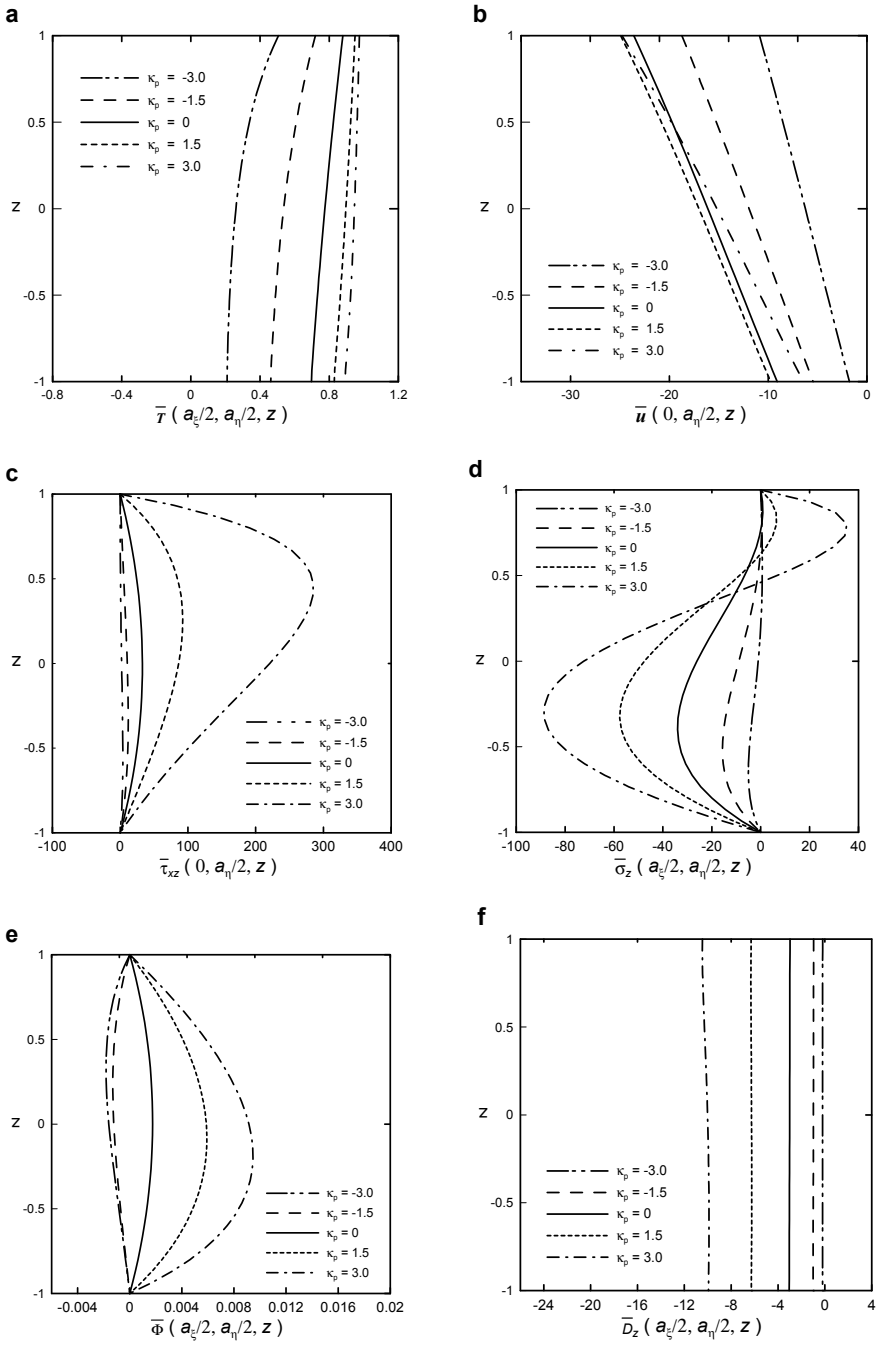

Figure 2: The through-thickness distributions of various field variables in an FG shell with the surface conditions of Case 1

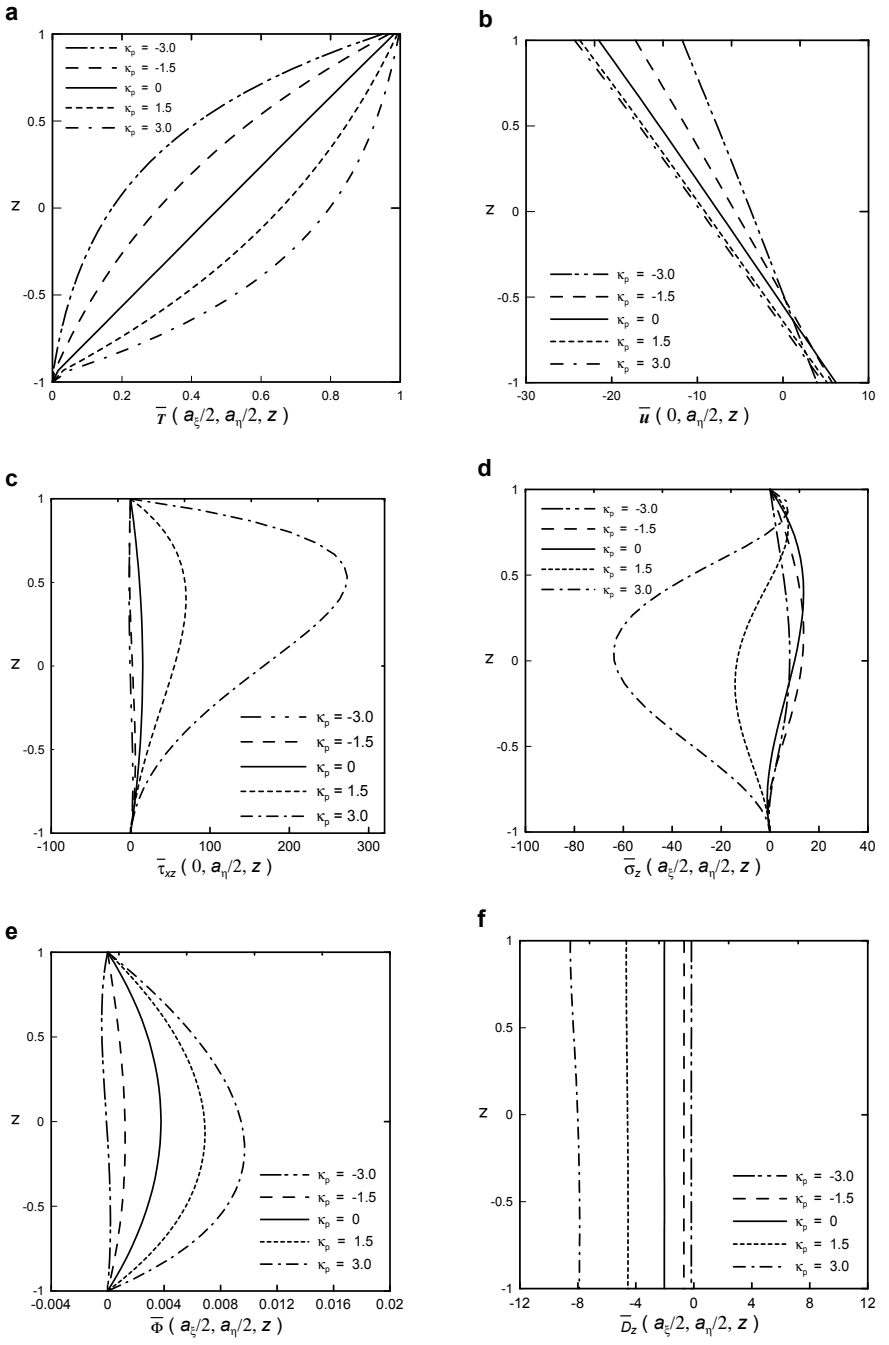

Figure 3: The through-thickness distributions of various field variables in an FG shell with the surface conditions of Case 2

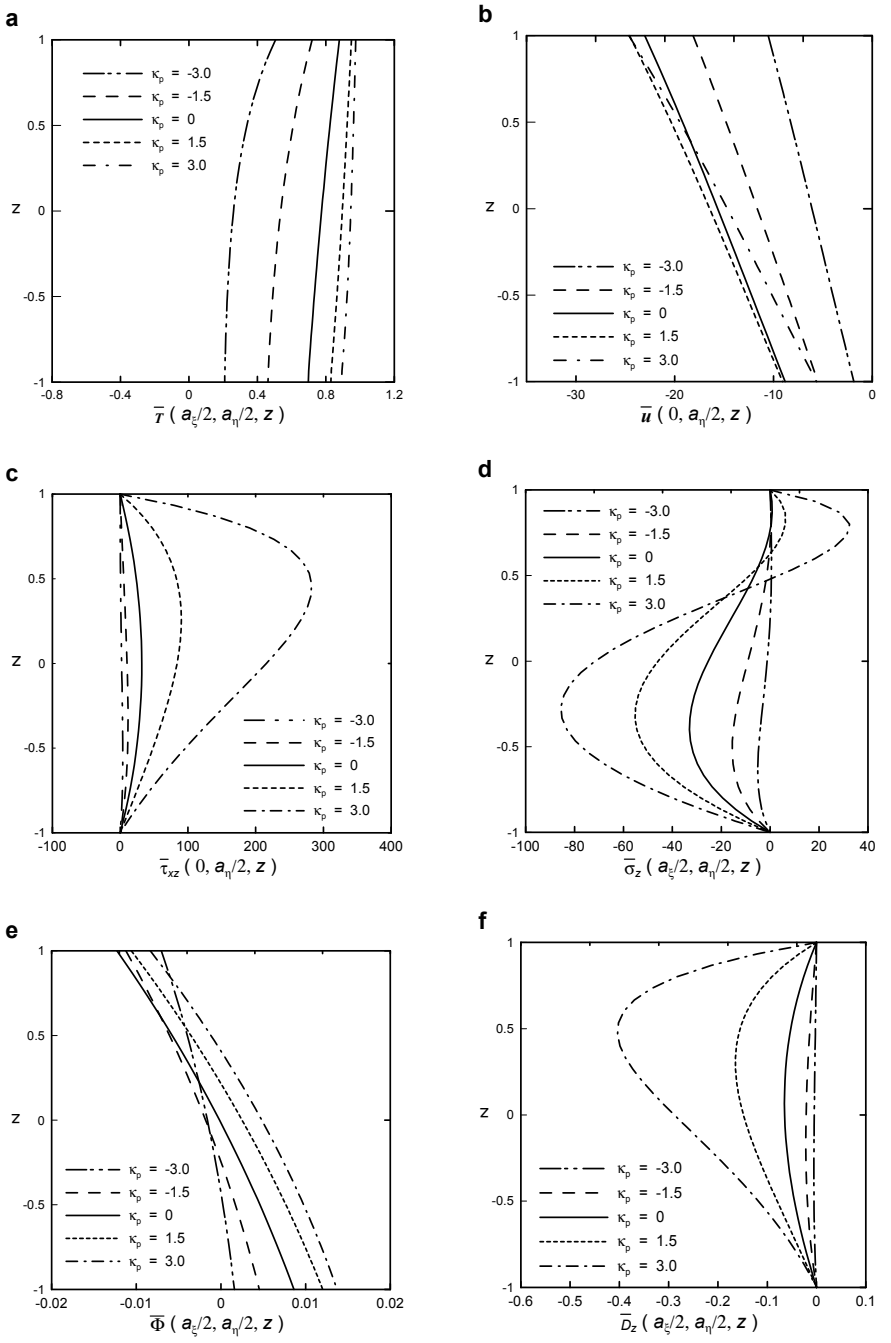

Figure 4: The through-thickness distributions of various field variables in an FG shell with the surface conditions of Case 3

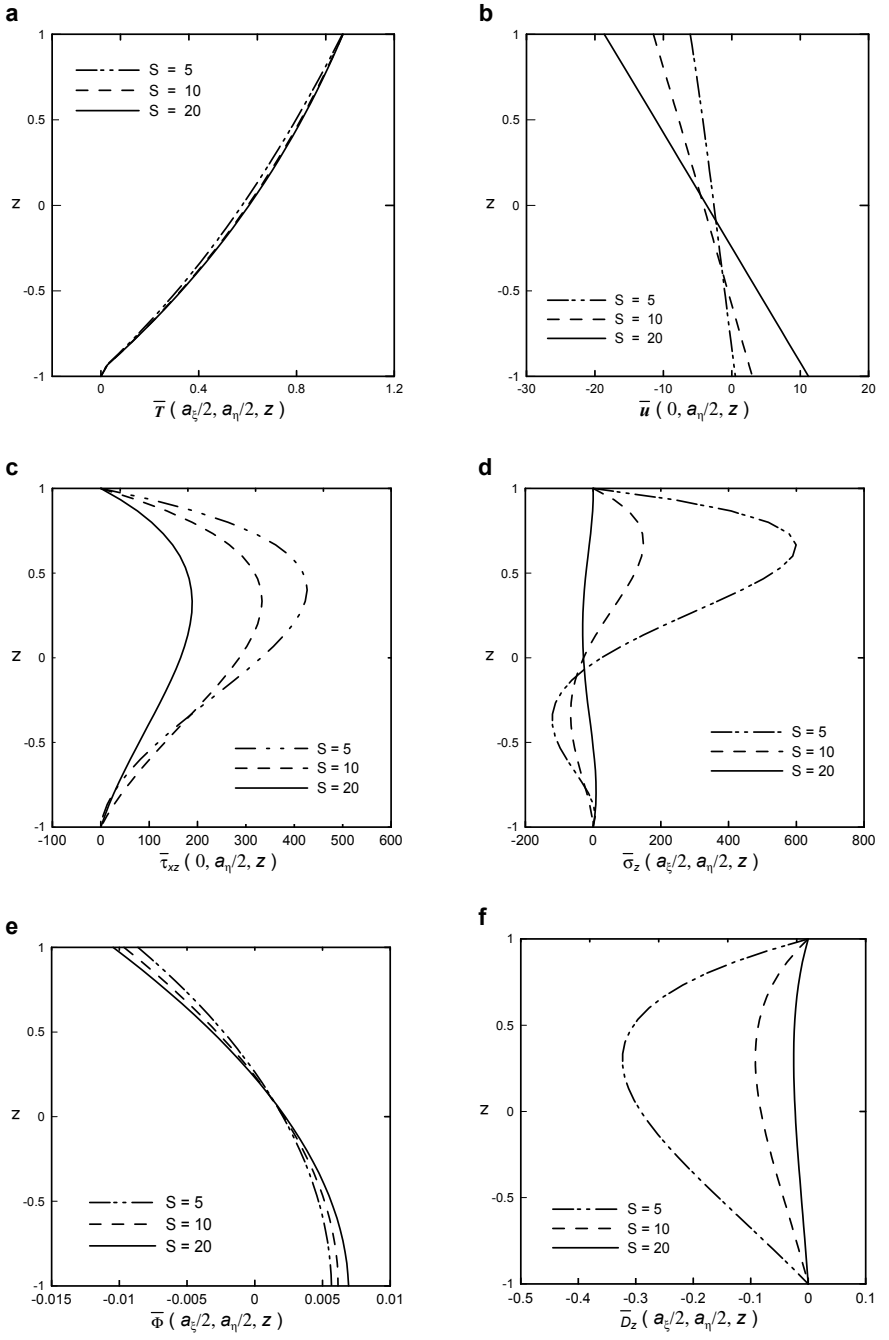

Figure 5: The variations of the through-thickness distributions of various field variables in an FG shell with the span-thickness ratio

6 Concluding remarks

In this paper we have developed a modified Pagano method for the three-dimensional coupled analysis of simply-supported, doubly curved FG piezo-thermo-elastic shells under thermal loads. Four different lateral surface conditions of the shells, namely closed-circuit and convection, closed-circuit and prescribed temperature, open-circuit and convection, as well as open-circuit and prescribed temperature surface conditions, are considered. The present formulation of the shells can be reduced to that of plates by letting the value of 1/curvature radius equal zero. In conjunction with a successive approximation method, an FG shell is modified as an *NL*-layered shell with an equal and small thickness, compared with the curvature radius, as well as the constant material properties in an average thickness sense for each layer. The accuracy and convergence rate of the present method are evaluated in comparison with the available 3D solutions, with which the present solutions are shown to converge rapidly and be in excellent agreement. In addition, the influence of the material-property gradient index on the variables in various fields, induced in the FG shells under the thermal load, is shown to be significant.

Acknowledgement: This work was supported by the National Science Council of the Republic of China through Grant NSC 97-2221-E006-128-MY3.

References

Ashida, F.; Tauchert, T.R. (2001): A general plane-stress solution in cylindrical coordinates for a piezothermoelastic plate. *International Journal of Solids and Structures*, vol. 38, pp. 4969–4985.

Chen, W.Q.; Ding, H.J.; Xu, R.Q. (2001): Three-dimensional static analysis of multilayered piezoelectric hollow spheres via the state space method. *International Journal of Solids and Structures*, vol. 38, pp. 4921–4936.

Chen, W.Q.; Lee, K.Y. (2003): Alternative state space formulations for magnetoelectric thermoelasticity with transverse isotropy and the application to bending analysis of nonhomogeneous plates. *International Journal of Solids and Structures*, vol. 40, pp. 5689–5705.

Crawley, E; Luis, J. (1987): Use of piezoelectric actuators as elements of intelligent structures. *AIAA Journal*, vol. 25, pp. 1373–1385.

Dube, G.P.; Kapuria, S.; Dumir, P.C. (1996a): Exact piezothermoelastic solution of simply-supported orthotropic flat panel in cylindrical bending. *International Journal of Mechanical Science*, vol. 38, pp. 1161–1177.

Dube, G.P.; Kapuria, S.; Dumir, P.C. (1996b): Exact piezothermoelastic solution

of simply-supported orthotropic circular cylindrical panel in cylindrical bending. *Archive of Applied Mechanics*, vol. 66, pp. 537–554.

Heyliger, P.; Brooks. S. (1995): Free vibration of piezoelectric laminates in cylindrical bending. *International Journal of Solids and Structures*, vol. 32, pp. 2945–2960.

Heyliger, P.; Brooks. S. (1996): Exact solutions for laminated piezoelectric plates in cylindrical bending. *Journal of Sound and Vibrations*, vol. 229, pp. 935–956.

Im, S.; Atluri, S.N. (1989): Effects of a piezo-actuator on a finitely deformed beam subjected to general loading. *AIAA Journal*, vol. 27, pp. 1801–1807.

Kapuria, S.; Dumir, P.C.; Sengupta, S. (1997): Exact axisymmetric solution for a simply supported piezoelectric cylindrical shell. *Archive of Applied Mechanics*, vol. 67, pp. 260–273.

Kapuria, S.; Sengupta, S.; Dumir, P.C. (1997): Three-dimensional solution for a hybrid cylindrical shell under axisymmetric thermoelectric load. *Archive of Applied Mechanics*, vol. 67, pp. 320–330.

Soldatos, K.P.; Hadjigeorgiou, V.P. (1990): Three-dimensional solution of the free vibration problem of homogeneous isotropic cylindrical shells and panels. *Journal of Sound Vibration*, vol. 137, pp. 369-384.

Tang, Y.Y.; Noor, A.K.; Xu, K. (1996): Assessment of computational models for thermoelectroelastic multilayered plates. *Computers & Structures*, vol. 61, 915–933.

Tauchert, T.R.; Ashida, F.; Noda, N.; Adali, S.; Verijenko, V. (2000): Developmemts in thermopiezoelasticity with relevance to smart composite structures. *Composite Structures*, vol. 48, pp. 31–38.

Tsai, Y.H.; Wu, C.P. (2008): Dynamic responses of functionally graded magneto-electro-elastic shells with open-circuit surface conditions. *International Journal of Engineering Science*, vol. 46, pp. 843–857.

Wu, C.P.; Chen, S.J.; Chiu, K.H. (2009): Three-dimensional static behavior of functionally graded magneto-electro-elastic plates using the modified Pagano method. *Mechanics Research Communications*, doi:10.1016/j.mechrescom.2009.10.003.

Wu, C.P.; Chiu, K.H.; Wang, Y.M. (2008): A review on the three-dimensional analytical approaches of multilayered and functionally graded piezoelectric plates and shells. *CMC: Computers, Materials, & Continua*, vol. 8, pp. 93–132.

Wu, C.P.; Liu, K.Y. (2007): A state space approach for the analysis of doubly curved functionally graded elastic and piezoelectric shells. *CMC: Computers, Materials, & Continua*, vol. 6, pp. 177–199.

Wu, C.P.; Lu, Y.C. (2009): A modified Pagano method for the 3D dynamic re-

sponses of functionally graded magneto-electro-elastic plates. *Composite Structures*, vol. 90, pp. 363–372.

Wu, C.P.; Syu, Y.S. (2006): Asymptotic solutions for multilayered piezoelectric cylinders under electromechanical loads. *CMC: Computers, Materials, & Continua*, vol. 4, pp. 87–108.

Wu, C.P.; Syu, Y.S. (2007): Exact solutions of functionally graded piezoelectric shells under cylindrical bending. *International Journal of Solids and Structures*, vol. 44, pp. 6450–6472.

Wu, C.P.; Syu, Y.S.; Lo, J.Y. (2007): Three-dimensional solutions for multilayered piezoelectric hollow cylinders by an asymptotic approach. *International Journal of Mechanical Sciences*, vol. 49, pp. 669–689.

Wu, C.P.; Tsai, Y.H. (2007): Static behavior of functionally graded magneto-electro-elastic shells under electric displacement and magnetic flux. *International Journal of Engineering Science*, vol. 45, pp. 744–769.

Wu, C.P.; Tsai, Y.H. (2009): Cylindrical bending vibration of functionally graded piezoelectric shells using the method of perturbation. *International Journal of Engineering Mathematics*, vol. 63, pp. 95–119.

Wu, X.H.; Shen, Y.P.; Chen, C. (2003): An exact solution for functionally graded piezothermoelastic cylindrical shell as sensors or actuators. *Materials Letters*, vol. 57, pp. 3532–3542.

Xu, K.; Noor, A.K.; Tang Y.Y. (1995): Three-dimensional solutions for coupled thermo-electro-elastic response of multilayered plates. *Computer Methods in Applied Mechanics and Engineering* , vol. 126, pp. 355–371.

Zhang, C.; Di, S.; Zhang, N. (2002): A new procedure for static analysis of thermo-electric laminated composite plates under cylindrical bending. *Composite Structures*, vol. 56, pp. 131–140.

Zhong, Z.; Shang, E.T. (2005): Exact analysis of simply supported functionally graded piezothermoelectric plates. *Journal of Intelligent Material Systems and Structures*, vol. 16, pp. 643–651.

Appendix A

The relevant coefficients of l_{ij} and k_{ij} in (17) and (18), respectively, are given by

$$\tilde{c}_{ij} = c_{ij}/Q, \quad \tilde{e}_{ij} = e_{ij}/e, \quad \tilde{\eta}_{ij} = \eta_{ij}Q/e^2;$$

$$Q_{ij} = c_{ij} - c_{i3}a_{1j} - e_{3i}a_{2j} \quad (i,j = 1,2,6), \quad \tilde{Q}_{ij} = Q_{ij}/Q;$$

$$a_{1k} = c_{k3}a_1 + e_{3k}a_2, \quad a_{2k} = c_{k3}b_1 + e_{3k}b_2, \quad a_{3k} = -\alpha_k + a_{1k}\alpha_3 - a_{2k}\beta_3 \quad (k = 1,2);$$

$$a_1 = \eta_{33}/\Delta, \quad a_2 = e_{33}/\Delta, \quad a_3 = \left(\eta_{33}\alpha_3 - e_{33}\beta_3\right)/\Delta,$$
$$b_1 = a_2, \quad b_2 = -c_{33}/\Delta, \quad b_3 = \left(e_{33}\alpha_3 + c_{33}\beta_3\right)/\Delta, \quad \Delta = c_{33}\eta_{33} + e_{33}^2. \tag{A.1}$$

Appendix B

The coefficients $\bar{l}_{ij}$ and $\bar{k}_{ij}$ in (30) and (31), respectively, are given by

$$\bar{l}_{12} = l_{12}, \quad \bar{l}_{21} = -\tilde{m}^2\left(\lambda_x h/\gamma_\xi^2 R\right) - \tilde{n}^2\left(\lambda_y h/\gamma_\eta^2 R\right), \quad \bar{l}_{22} = l_{22},$$

$$\bar{k}_{11} = k_{11}, \quad \bar{k}_{15} = k_{15}, \quad \bar{k}_{17} = -\tilde{m}\left(\tilde{e}_{15} h/\tilde{c}_{55}\gamma_\xi R\right), \quad \bar{k}_{18} = -\tilde{m}\left(1/\gamma_\xi\right),$$
$$\bar{k}_{22} = k_{22}, \quad \bar{k}_{26} = k_{26}, \quad \bar{k}_{27} = -\tilde{n}\left(\tilde{e}_{24} h/\tilde{c}_{44}\gamma_\eta R\right), \quad \bar{k}_{28} = -\tilde{n}/\gamma_\eta,$$
$$\bar{k}_{33} = k_{33}, \quad \bar{k}_{37} = -\tilde{m}^2\left[\left(\tilde{e}_{15}^2/\tilde{c}_{55} + \tilde{\eta}_{11}\right) h/\gamma_\xi^2 R\right] - \tilde{n}^2\left[\left(\tilde{e}_{24}^2/\tilde{c}_{44} + \tilde{\eta}_{22}\right) h/\gamma_\eta^2 R\right],$$
$$\bar{k}_{41} = -\tilde{m}\left[\left(\tilde{Q}_{11}/\gamma_\xi^2 R_x\right) + \left(\tilde{Q}_{21}/\gamma_\xi\gamma_\eta R_y\right)\right],$$
$$\bar{k}_{42} = -\tilde{n}\left[\left(\tilde{Q}_{12}/\gamma_\xi\gamma_\eta R_x\right) + \left(\tilde{Q}_{22}/\gamma_\eta^2 R_y\right)\right],$$
$$\bar{k}_{43} = k_{43}, \quad \bar{k}_{44} = k_{44}, \quad \bar{k}_{48} = k_{48}, \quad \bar{k}_{49} = k_{49},$$
$$\bar{k}_{51} = \tilde{m}^2\left(\tilde{Q}_{11}/\gamma_\xi^2\right) + \tilde{n}^2\left(\tilde{Q}_{66}/\gamma_\eta^2\right), \quad \bar{k}_{52} = \tilde{m}\tilde{n}\left(\tilde{Q}_{12} + \tilde{Q}_{66}\right)/\left(\gamma_\xi\gamma_\eta\right),$$
$$\bar{k}_{53} = -\tilde{m}\left(a_{21} e/Q\gamma_\xi\right), \quad \bar{k}_{54} = -\tilde{m}\left(a_{11} h/R\gamma_\xi\right), \quad \bar{k}_{55} = k_{55},$$
$$\bar{k}_{58} = -\tilde{m}\left[\left(\tilde{Q}_{11}/\gamma_\xi^2 R_x\right) + \left(\tilde{Q}_{12}/\gamma_\xi\gamma_\eta R_y\right)\right], \quad \bar{k}_{59} = -\tilde{m}\left(a_{31}/\gamma_\xi\alpha_t\right),$$
$$\bar{k}_{61} = \tilde{m}\tilde{n}\left[\left(\tilde{Q}_{21} + \tilde{Q}_{66}\right)/\gamma_\xi\gamma_\eta\right], \quad \bar{k}_{62} = \tilde{m}^2\left(\tilde{Q}_{66}/\gamma_\xi^2\right) + \tilde{n}^2\left(\tilde{Q}_{22}/\gamma_\eta^2\right),$$
$$\bar{k}_{63} = -\tilde{n}\left(a_{22} e/Q\gamma_\eta\right),$$
$$\bar{k}_{64} = -\tilde{n}\left(a_{12} h/R\gamma_\eta\right), \quad \bar{k}_{66} = k_{66},$$
$$\bar{k}_{68} = -\tilde{n}\left[\left(\tilde{Q}_{21}/\gamma_\xi\gamma_\eta R_x\right) + \left(\tilde{Q}_{22}/\gamma_\eta^2 R_y\right)\right], \quad \bar{k}_{69} = -\tilde{n}\left(a_{32}/\gamma_\eta\alpha_t\right),$$
$$\bar{k}_{73} = k_{73}, \quad \bar{k}_{74} = k_{74}, \quad \bar{k}_{78} = k_{78}, \quad \bar{k}_{79} = k_{79},$$
$$\bar{k}_{84} = k_{84}, \quad \bar{k}_{88} = k_{88}, \quad \bar{k}_{89} = k_{89}. \tag{B.1}$$